Author version: *Nat. Geosci., vol.10; 2017; 24-29*

# $N_2$ production rates limited by nitrite availability in the Bay of Bengal oxygen minimum zone

L.A. Bristow[1,2]*, C.M. Callbeck[2]*, M. Larsen[1]*, M.A. Altabet[3], J. Dekaezemacker[2], M. Forth[1], M. Gauns[4], R.N. Glud[1], M.M.M. Kuypers[2], G. Lavik[2], J. Milucka[2], S.W.A. Naqvi[4], A. Pratihary[4], N.P. Revsbech[5], B. Thamdrup[1], A.H. Treusch[1], D.E. Canfield[1,6]

*these authors contributed equally to the work

[1] Department of Biology and Nordic Center for Earth Evolution (NordCEE), University of Southern Denmark, Campusvej 55, 5230 Odense M, Denmark.

[2] Max Planck Institute for Marine Microbiology, Celsiusstrasse 1, 28359 Bremen, Germany.

[3] School for Marine Science and Technology, University of Massachusetts Dartmouth, 706 South Rodney French Blvd, New Bedford, MA 02744-1221, USA.

[4] CSIR-National Institute of Oceanography, Dona Paula, 403 004, Goa, India,

[5] Department of Biological Sciences, Aarhus University, Building 1540, DK-8000 Aarhus C, Denmark.

[6] Corresponding author; dec@biology.sdu.dk

**A third or more of the fixed nitrogen lost from the oceans as $N_2$ is removed by anaerobic microbial processes in open ocean oxygen minimum zones. These zones have expanded over the past decades, and further anthropogenically-induced expansion could accelerate nitrogen loss. However, in the Bay of Bengal there has been no indication of nitrogen loss, although oxygen levels are below the detection level of conventional methods (1 to 2 μM). Here we quantify the abundance of microbial genes associated with $N_2$ production, measure nitrogen transformations in incubations of sampled seawater with isotopically labeled nitrogen compounds, and analyse geochemical signatures of these processes in the water column. We find that the Bay of Bengal supports denitrifier and anammox microbial populations, mediating low, but significant N loss. Yet, unlike other oxygen minimum zones, our measurements using a highly sensitive oxygen sensor demonstrate that the Bay of Bengal has persistent concentrations of oxygen in the 10 to 200 nM range. We propose that this oxygen supports nitrite oxidation, thereby restricting the nitrite available for anammox or denitrification. If these traces of oxygen were removed, nitrogen loss in the Bay of Bengal oxygen minimum zone waters could accelerate to global significance.**

Oxygen deficient regions of the open ocean account for 20 to 40% of fixed nitrogen loss, while making up only approximately 1% ($O_2$ < 20 μM) of global ocean volume[1]. Regions of nitrogen loss associated with oxygen depletion are presently recognized in the Eastern Tropical Pacific Ocean, off the coast of Namibia, and in the Arabian Sea[1, 2, 3]. In this regard the Bay of Bengal (BoB) has proven an enigma, with no clear evidence for nitrogen loss despite oxygen depletion (< 2 μM $O_2$;[4]), although only geochemical indicators of nitrogen loss have been investigated to date in this region[4, 5, 6].

We sampled the BoB in January 2014 during the winter monsoon (Figure 1 and S1). At five stations we measured oxygen *in situ* with a highly sensitive STOX sensor (switchable trace oxygen)[7, 8], with a limit of detection (LOD) of 7 to 12 nM. We used Niskin bottles to collect samples for nutrients, dissolved gases, nitrate isotopic analyses, molecular characterization of microbial populations and for experiments exploring aerobic and anaerobic microbial nitrogen metabolism.

**Oxygen levels and microbial populations in Bay of Bengal**

STOX oxygen data revealed sub-micromolar oxygen concentrations over a depth interval of about 200 meters throughout the study area (Figure 1). Only six single measurements were below the LOD, and these were confined to thin layers in the depth range between 280 and 360 m at Station 7 (Table S1). There was no evidence for distinct broad anoxic zones as seen in the other OMZs at any station, even at Station 1, where a secondary nitrite maximum of up to 180 nM was observed in the depth range 115 m to 150 m (Figure 1a; nitrite was at or below the LOD of 10 nM at all other stations analyzed). At this station, the lowest oxygen concentration was 36 nM at ~150 m (Figure 1 and Table S1). Persistent oxygen and low nitrite in the BoB contrasts with other major OMZs, which have anoxic cores (oxygen below STOX sensor detection) with > 500 nM nitrite[9, 10]. When calibrated to the STOX data (Figure S2), a Seabird oxygen sensor revealed tremendous vertical structure in the oxygen profiles (Figure 1), indicating oxygen input by lateral intrusions.

Despite the lack of evidence for anoxia in BoB OMZ waters, the vertical zonation of microorganisms with nitrogen-metabolizing capabilities resembled typical OMZs supporting active $N_2$ production as indicated by 16S rRNA and functional gene abundances (Figure 2). Anammox bacteria, as quantified through their nitrite reductase gene (*Scalindua nirS*, or Sc *nirS*), were present within the OMZ waters, peaking at the depth of 150 m with about 1300 copies $mL^{-1}$, some 40 to 60% of the maximal abundance found in other OMZs with active $N_2$ production[11, 12]. Nitrite reductase genes attributed to denitrifiers (Denitrifier *nirS*) were found at similar distribution and abundance to the Sc *nirS*, and were

even more abundant than in the Eastern Tropical South Pacific (ETSP) OMZ[11, 13]. In addition, the distribution of functional genes of aerobic ammonium and nitrite oxidizers, thaumarchaeotal *amoA* (Th *amoA*) and *Nitrospira/Nitrospina nxrB* (*nxrB*) respectively, resembled the distributions in other OMZ waters[11, 13, 14, 15], where Th *amoA* abundance peaks in the upper oxycline, here at about 80 m, and *nxrB* abundance peaks lower in the water column where Sc *nirS* is also most abundant. The similarity with other OMZs was further supported by the presence of the SUP05 clade, gammaproteobacterial sulfur oxidizers (GSO), and abundant adenylylsulfate (APS) reductase genes (*aprA*), suggesting a role for sulfur cycling in the BoB OMZ waters[16] (Figure S3).

**Activity of microbial nitrogen transformations**

Thus, microbial populations in BoB OMZ waters are capable of both anaerobic and aerobic nitrogen (and maybe sulfur) cycling as in other OMZs supporting $N_2$ production, despite a lack of any prior evidence for $N_2$ production. We performed parallel experiments with $^{15}N$-labeling to survey rates of microbial nitrate reduction and $N_2$ production in BoB OMZ waters (process rate experiments). With additions of $^{15}NH_4^+$ alone, anammox ($NH_4^+ + NO_2^- \rightarrow N_2 + 2H_2O$) rates were below detection (LOD 1.3 nM N $d^{-1}$) at all stations. Anammox rates of up to 6.2 nM N $d^{-1}$, however, were observed when $NH_4^+$ and $NO_2^-$ were added together, with labeling of either of the substrates (Figure 3a and S4). These potential rates are comparable to off-shore locations in the OMZs of the ETSP[13] and Eastern Tropical North Pacific (ETNP)[17].

Anammox was also detected at rates of up to 5.5 nM N $d^{-1}$ in separate experiments designed to explore the oxygen regulation of nitrite transformations (oxygen regulation experiments) where $^{15}NO_2^-$ was added alone (Figure 3b). Anammox activity decreased with increasing oxygen concentrations in three of the four experiments, but activity was observed up to our maximum concentration of 9.5 μM, in line with a number of previous observations[18]. Indeed, anammox rates remained high across the oxygen concentrations of the BoB OMZ. Summarizing our results, anammox was not measurable when ammonium was added alone, but was only detected with added nitrite. Thus, there is a large potential for N-loss via anammox in the BoB, but *in situ* anammox bacteria are likely nitrite-limited rather than being limited by ammonium or inhibited by oxygen. Denitrification was below the LOD (2.7 nM N $d^{-1}$) in BoB OMZ waters in our process rate experiments (Figure 3A). We did, however, detect denitrification (up to 0.9 nM N $d^{-1}$) with $^{15}NO_2^-$ at Station 5 (but not Stations 1 or 4) in our oxygen regulation experiments with a lower median detection limit of 0.4 nM N $d^{-1}$ (Figure 3b), suggesting a patchy

distribution of denitrification in BoB OMZ waters. When present, denitrification exhibited higher oxygen sensitivity than anammox (Figure 3b), with complete inhibition at $O_2$ concentrations above 4-5 μM (with a single point deviating from this trend), consistent with observations from the ETSP OMZ[19].

Despite the low rates of anammox and denitrification, and the general absence of nitrite in BoB OMZ waters, we measured nitrite production rates from nitrate ($^{15}NO_3^-$) of up to 12.1 nM N $d^{-1}$ at Stations 4 and 5 (Figure 3a). We also measured potential nitrite oxidation rates of up to 52 nM N $d^{-1}$ in our oxygen regulation experiments (Figure 3b; Table S2). The presence of nitrite-oxidizing bacteria was confirmed by the detection of *Nitrospira/Nitrospina*-related *nxrB* sequences (Figure 2). The rates of nitrite oxidation exceeded those of nitrite production even at low oxygen concentrations, reaching maximum values at ~1 μM $O_2$, suggesting nitrite oxidizing bacteria have a high affinity for oxygen (Figure 3a) in agreement with recent observations[20]. Our combined data indicate an active, coupled, anaerobic/aerobic nitrogen cycle where nitrate is reduced to nitrite and rapidly oxidized again to nitrate in the OMZ waters. A close coupling between nitrate reduction to nitrite and subsequent nitrite oxidation has also been described in the oxyclines of other OMZs, where nitrite also fails to accumulate despite active nitrate reduction to nitrite[18, 21].

Thus, based on our experimental data, we conclude that the BoB OMZ oxygen concentrations (10 to 200 nM) limit $N_2$ production through anammox indirectly, by enabling aerobic nitrite oxidizing bacteria to outcompete anammox bacteria for the available nitrite. Denitrification was also not inhibited by the oxygen levels of BoB OMZ waters, but was generally low and only detected at two stations. Such patchiness may be related to the presence or absence of organic-matter rich aggregates in the incubations[17].

**Geochemical evidence of nitrogen cycling**

Our molecular results and process rate measurements are supported by geochemical data that indicate a slow, but functioning, anaerobic nitrogen cycle in BoB OMZ waters. A small, albeit noisy, nitrogen deficit of 2 to 3 μM, indicative of net N loss, was calculated from our nutrient data (Figure 4 and Table S4). We also observed a maximum $N_2$ excess (calculated from $N_2$/Ar ratios) on the order of 2 to 3 μM $N_2$ in the OMZ waters (equivalent to 4 to 6 μM N). Throughout the sub-surface ocean, $N_2$ excess increases monotonically with depth due to abiotic factors[22] but a local maximum within OMZs is strongly indicative of biogenic $N_2$ production[23]. The $\delta^{15}N$ of $NO_3^-$ from the BoB OMZ showed small

enrichments of up to 1.5 ‰ relative to deep-water values consistent with net nitrate reduction. The larger $^{18}O$ enrichment in $NO_3^-$ of 3 ‰ is consistent with the coupled anaerobic/aerobic nitrogen cycle explored above, with nitrate reduction to nitrite followed by reoxidation back to nitrate[24] (see SI). These three geochemical indicators integrate over larger water volumes and over longer time scales than our rate measurements, and, therefore, imply that nitrogen cycling and $N_2$ production are persistent phenomena in the BoB, although these signals are smaller in magnitude than in other major OMZs[23, 24].

Taken together, our nitrogen deficit and $N_2$ excess measurements point to ~2 μM of biologically produced $N_2$ (4 μM $N_2$-N) in BoB OMZ waters. Previous studies have estimated annual water exchange of $18\times10^{12}$ $m^3$ $y^{-1}$ in the depth interval from 150 to 250 meters, and $31\times10^{12}$ $m^3$ $y^{-1}$ in the interval from 250 to 500 m[25]. We take 40% of the latter ($12\times10^{12}$ $m^3$ $y^{-1}$) to estimate the exchange from 250 to 350 m, obtaining a total annual water exchange of $30\times10^{12}$ $m^3$ $y^{-1}$ from 150 to 350 meters depth, and a turnover time of 12 years for the $372\times10^{12}$ $m^3$ volume of this interval[25]. This exchange rate, combined with a biogenic $N_2$ excess of 2 μM, yields an annual production rate of ~1.7 Tg N $y^{-1}$. This $N_2$ production is about 12% of the production rate in the Arabian Sea, and some 2.5 % of the global water-column production in OMZ settings (66±6 Tg N $y^{-1}$)[26].

This annual rate of $N_2$ production amounts to an average $N_2$ production rate of 0.88 nM-N $d^{-1}$ for the volume between 150 to 350 m. As we were unable to measure $N_2$ production by anammox without added nitrite, and as denitrification rates were low when detected at all (Figure 3), there must be either seasonal or spatial variability in $N_2$ production that we have not captured in our process rate experiments. Still, our process rate and oxygen regulation experiments (Figure 3) suggest a potential for $N_2$ production of about 3 nM-N $d^{-1}$ under nitrite replete conditions, some 3.5 times greater than the average rate calculated from the $N_2$ excess. Therefore, there is considerable potential for additional $N_2$ production in the BoB OMZ above that indicated from the geochemical indicators. As $N_2$ production, particularly through anammox, is nitrite limited, the rates should increase if oxygen is depleted further, suppressing nitrite oxidation and allowing nitrite to accumulate[9] in BoB OMZ waters. An accumulation of nitrite in the sub-micromolar range may be sufficient to stimulate anammox substantially, judging from the independence of anammox rates on nitrite concentrations across OMZs[27] . If $N_2$ production increased to an average of 3 nM-N $d^{-1}$ (as our experiments suggest), then $N_2$ production rates would increase to about 6 Tg N $y^{-1}$ or about 40% of Arabian Sea rates and 9% of global water-column rates[26]. Such an increase would make the BoB an important player in the global nitrogen cycle.

**The Bay of Bengal at a tipping point**

The stable accumulation of nitrite in BoB OMZ waters would require the removal of the last traces of oxygen. The oxygen concentration reflects the dynamic balance between the processes mixing oxygen into the OMZ and the processes consuming it. An increase in the flux of organic matter to the OMZ waters would be one way to increase oxygen consumption, and an increase in primary production could accomplish this. Possible vehicles for increased primary production include the accelerated input of anthropogenic nitrogen into the BoB, as projected for the coming decades[28] and changing intensity of the summer monsoon. In particular, the high southwesterly summer monsoon winds generate coastal upwelling, producing high concentrations of chlorophyll *a*[29] and enhanced oxygen depletion in coastal waters[30]. Therefore, accelerated summer monsoon intensity could potentially increase the flux of organic matter to OMZ waters, drawing down oxygen and accelerating $N_2$ production.

However, an enhanced summer monsoon would also increase river runoff and the flux of particulates to the BoB. Riverine particulates ballast sinking organic material resulting in rapid sedimentation of labile organics through the OMZ, reducing their decomposition in OMZ waters[6]. Thus, the main climate driver in the BoB, the summer monsoon, generates what appear to be opposing influences on the development of anoxia in the BoB OMZ waters. A test of summer monsoon intensity on $N_2$ loss in the BoB could come from current climate change as some climate models suggest future increases in the intensity of the Asian summer monsoon[31].

Historical evidence indeed suggests a potential relationship between climate change and an active anaerobic nitrogen cycle in the BoB[32]. Elevated sediment nitrogen isotope values are correlated with elevated concentrations of organic matter and organic nitrogen about 42,000 years ago. These results suggest that higher rates of organic matter productivity at that time enabled a nitrogen cycle with higher N loss rates, although the driver of this relationship is unclear.

Overall, we demonstrate that the BoB is like the other well known OMZs with microbial populations supporting $N_2$ production, although at low rates. The BoB OMZ also maintains widespread nanomolar oxygen concentrations that inhibit the stable accumulation of nitrite, a key substrate for N-loss. If these last traces of oxygen were removed, allowing nitrite to accumulate, rates of $N_2$ production would increase considerably. Thus, the BoB OMZ sits at a geochemical "tipping point" where any process removing the last of the oxygen, such as anthropogenic nutrient input or climate change, would make the BoB a major player in the marine nitrogen cycle.

## References


1. Codispoti LA, Brandes JA, Christensen JP, Devol AH, Naqvi SWA, Paerl HW*, et al.* The oceanic fixed nitrogen and nitrous oxide budgets: Moving targets as we enter the anthropocene? *Scientia Marina* 2001, **65:** 85-105.
2. Kuypers MMM, Lavik G, Woebken D, Schmid M, Fuchs BM, Amann R*, et al.* Massive nitrogen loss from the Benguela upwelling system through anaerobic ammonium oxidation. *Proceedings of the National Academy of Sciences of the United States of America* 2005, **102**(18)**:** 6478-6483.
3. Ulloa O, Canfield DE, DeLong EF, Letelier RM, Stewart FJ. Microbial oceanography of anoxic oxygen minimum zones. *Proceedings of the National Academy of Sciences of the United States of America* 2012, **109**(40)**:** 15996-16003.
4. Naqvi WSA, Narvekar PV, Desa E. Coastal biogeochemical processes in the North Indian Ocean. In: Robinson AR, Brink KH (eds). *The Sea*, vol. 14, 2005.
5. Sarma V, Krishna MS, Viswanadham R, Rao GD, Rao VD, Sridevi B*, et al.* Intensified oxygen minimum zone on the western shelf of Bay of Bengal during summer monsoon: influence of river discharge. *Journal of Oceanography* 2013, **69**(1)**:** 45-55.
6. Rao CK, Naqvi SWA, Kumar MD, Varaprasad SJD, Jayakumar DA, George MD*, et al.* Hydrochemistry of the bay of Bengal-possible reasons for a different water-column cycling of carbon and nitrigen from the Arabian Sea. *Marine Chemistry* 1994, **47**(3-4)**:** 279-290.
7. Revsbech NP, Larsen LH, Gundersen J, Dalsgaard T, Ulloa O, Thamdrup B. Determination of ultra-low oxygen concentrations in oxygen minimum zones by the STOX sensor. *Limnology and Oceanography: Methods* 2009, **7:** 371-381.
8. Larsen M, Lehner P, Borisov SM, Klimant I, Fischer JP, Stewart FJ*, et al.* In situ quantification of ultra-low O2 concentrations in oxygen minimum zones: Application of novel optodes. *Limnology and Oceanography: Methods* 2016**:** n/a-n/a.
9. Thamdrup B, Dalsgaard T, Revsbech NP. Widespread functional anoxia in the oxygen minimum zone of the Eastern South Pacific. *Deep-Sea Research Part I-Oceanographic Research Papers* 2012, **65:** 36-45.
10. Tiano L, Garcia-Robledo E, Dalsgaard T, Devol AH, Ward BB, Ulloa O*, et al.* Oxygen distribution and aerobic respiration in the north and south eastern tropical Pacific oxygen minimum zones. *Deep-Sea Research Part I-Oceanographic Research Papers* 2014, **94:** 173-183.

11. Lam P, Lavik G, Jensen MM, van de Vossenberg J, Schmid M, Woebken D*, et al.* Revising the nitrogen cycle in the Peruvian oxygen minimum zone. *Proceedings of the National Academy of Sciences of the United States of America* 2009, **106**(12)**:** 4752-4757.
12. Jensen MM, Lam P, Revsbech NP, Nagel B, Gaye B, Jetten MSM*, et al.* Intensive nitrogen loss over the Omani Shelf due to anammox coupled with dissimilatory nitrite reduction to ammonium. *Isme J* 2011, **5**(10)**:** 1660-1670.
13. Kalvelage T, Lavik G, Lam P, Contreras S, Arteaga L, Loscher CR*, et al.* Nitrogen cycling driven by organic matter export in the South Pacific oxygen minimum zone. *Nature Geoscience* 2013, **6**(3)**:** 228-234.
14. Beman JM, Shih JL, Popp BN. Nitrite oxidation in the upper water column and oxygen minimum zone of the eastern tropical North Pacific Ocean. *Isme Journal* 2013, **7**(11)**:** 2192-2205.
15. Beman JM, Popp BN, Alford SE. Quantification of ammonia oxidation rates and ammonia-oxidizing archaea and bacteria at high resolution in the Gulf of California and eastern tropical North Pacific Ocean. *Limnology and Oceanography* 2012, **57**(3)**:** 711-726.
16. Canfield DE, Stewart FJ, Thamdrup B, De Brabandere L, Dalsgaard T, Delong EF*, et al.* A cryptic sulfur cycle in oxygen-minimum-zone waters off the Chilean Coast. *Science* 2010, **330:** 1375-1378.
17. Ganesh S, Bristow LA, Larsen M, Sarode N, Thamdrup B, Stewart FJ. Size-fraction partitioning of community gene transcription and nitrogen metabolism in a marine oxygen minimum zone. *The ISME Journal* 2015.
18. Kalvelage T, Jensen MM, Contreras S, Revsbech NP, Lam P, Gunter M*, et al.* Oxygen Sensitivity of Anammox and Coupled N-Cycle Processes in Oxygen Minimum Zones. *Plos One* 2011, **6**(12).
19. Dalsgaard T, Stewart FJ, Thamdrup B, De Brabandere L, Revsbech NP, Ulloa O*, et al.* Oxygen at Nanomolar Levels Reversibly Suppresses Process Rates and Gene Expression in Anammox and Denitrification in the Oxygen Minimum Zone off Northern Chile. *Mbio* 2014, **5**(6).
20. Bristow LA, Dalsgaard T, Tiano L, Mills DB, Bertagnolli AD, Wright JJ*, et al.* Ammonium and nitrite oxidation at nanomolar oxygen concentrations in oxygen minimum zone waters. *Proceedings of the National Academy of Sciences* 2016, **113**(38)**:** 10601-10606.
21. Füssel J, Lam P, Lavik G, Jensen MM, Holtappels M, Gunter M*, et al.* Nitrite oxidation in the Namibian oxygen minimum zone. *Isme Journal* 2012, **6**(6)**:** 1200-1209.
22. Hamme RC, Emerson SR. Mechanisms controlling the global oceanic distribution of the inert gases argon, nitrogen and neon. *Geophysical Research Letters* 2002, **29**(23).

23. Chang BX, Devol AH, Emerson SR. Fixed nitrogen loss from the eastern tropical North Pacific and Arabian Sea oxygen deficient zones determined from measurements of N-2:Ar. *Global Biogeochemical Cycles* 2012, **26**.

24. Casciotti KL, Buchwald C, McIlvin M. Implications of nitrate and nitrite isotope measurements for the mechanisms of nitrogen cycling in the Peru oxygen deficient zone. *Deep-C Research I* 2013, **80:** 78-93.

25. Sarma VVSS. An evaluation of physical and biogeochemical processes regulating perennial suboxic conditions in the water column of the Arabian Sea. *Global Biogeochemical Cycles* 2002, **16**(4)**:** 1082, doi:1010.1029/2001GB001461.

26. DeVries T, Deutsch C, Primeau F, Chang B, Devol A. Global rates of water-column denitrification derived from nitrogen gas measurements. *Nature Geoscience* 2012, **5**(8)**:** 547-550.

27. Lam P, Kuypers MMM. Microbial Nitrogen Cycling Processes in Oxygen Minimum Zones. *Annual Review of Marine Science* 2011, **3**(1)**:** 317-345.

28. Duce RA, LaRoche J, Altieri K, Arrigo KR, Baker AR, Capone DG*, et al.* Impacts of atmospheric anthropogenic nitrogen on the open ocean. *Science* 2008, **320**(5878)**:** 893-897.

29. Gomes HR, Goes JI, Saino T. Influence of physical processes and freshwater discharge on the seasonality of phytoplankton regime in the Bay of Bengal. *Continental Shelf Research* 2000, **20**(3)**:** 313-330.

30. Sardessai S, Ramaiah N, Kumar SP, de Sousa SN. Influence of environmental forcings on the seasonality of dissolved oxygen and nutrients in the Bay of Bengal. *Journal of Marine Research* 2007, **65**(2)**:** 301-316.

31. Turner AG, Annamalai H. Climate change and the South Asian summer monsoon. *Nature Climate Change* 2012, **2**(8)**:** 587-595.

32. Pattan JN, Mir IA, Parthiban G, Karapurkar SG, Matta VM, Naidu PD*, et al.* Coupling between suboxic condition in sediments of the western Bay of Bengal and southwest monsoon intensification: A geochemical study. *Chemical Geology* 2013, **343:** 55-66.

## Additional Information

Correspondence and requests for materials should be addressed to D.E.C (dec@biology.sdu.dk)

## Acknowledgments

We thank the captain and crew of the *RV Sagar Kanya* for their support during sampling. We are grateful to A. Glud, G. Klockgether, J. Larkum, L. Piepgras, P. Sørensen for technical and analytical assistance. This study was supported by the Danish National Research Foundation (DNRF53), European Research Council 'Oxygen' grant (267233), and the Max Planck Society. We gratefully acknowledge the Ministry of Earth Sciences (MoES), INDIA for funding the research through the SIBER (INDIA) project GAP2425 and for making *RV Sagar Kanya* available for this work. J.D. was supported by the Sonderforschungsbereiche (SFB754) GEOMAR, Kiel and C.M.C by a scholarship from the Natural Sciences and Engineering Research Council of Canada (NSERC).

## Author Contributions

L.A.B., M.L., M.G., R.N.G., M.M.M.K., G.L., S.W.A.N., N.P.R., B.T. and D.E.C. designed the study; L.A.B., C.M.C., M.L., J.D., M.F., G.L., J. M., D.E.C. performed experiments; L.A.B., C.M.C., M.L., M.A.A., M.F., G.L., B.T., A.H.T. and D.E.C. analyzed data; A.P. provided nutrient data; L.A.B., C.M.C., M.L., R.N.G., G.L., B.T. and D.E.C. wrote the manuscript with input from all co-authors.

## Competing Financial Interests

The authors declare no competing financial interests in association with this study.

**Figure Captions**

**Figure 1. Station locations and oxygen data for the Bay of Bengal**. Oxygen concentration profiles focus on the upper 500 m of the water column containing the oxygen minimum zone (OMZ). Black dots represent STOX oxygen data, while the blue line represents Seabird oxygen data, calibrated with the STOX data at the low oxygen levels. At Station 1 (a), nitrite concentrations are indicated by the red line (a distinct primary nitrite maximum in the oxic upper 100m, and a secondary nitrite maximum under nanomolar oxygen concentrations). Nitrite was not detected at any of the other stations.

**Figure 2. Abundance of bacterial 16S rRNA and selected functional genes in the Bay of Bengal**. Copy numbers were obtained with qPCR using primer sets as shown in Table S3. Shown are total copies of bacterial 16S rRNA (a), nitrite reductase genes attributed to denitrifiers (Denitrifier *nirS*; b) and to anammox bacteria (*Scalindua*, Sc *nirS*; c), thaumarchaeotal ammonia monooxygenase (Th *amoA*; d) and *Nitrospira/Nitrospina* nitrite oxidoreductase (*nxrB*; e). The dashed rectangle outlines the approximate depth interval where oxygen concentrations drop below 2.5 µM. Error bars represent the standard deviation. Note variability in x axes scales.

**Figure 3. Depth profiles and regulation experiments of N transformations in the Bay of Bengal** a) Process rate experiments showing rates of anammox and nitrate reduction to nitrite using $^{15}N$ labeling experiments. Denitrification was below detection in these experiments: b) Experiments using $^{15}N$-labeled nitrite to explore the oxygen regulation of nitrogen transformations. The top panel shows the oxygen regulation of nitrite oxidation (note the use of both y axes), the middle panel shows the oxygen regulation of denitrification, while the bottom panel shows the oxygen regulation of anammox. Error bars represent the standard error.

**Figure 4. Geochemical indicators of nitrogen cycling in the Bay of Bengal OMZ waters.** Depth profiles of excess $N_2$ (calculated from $N_2$/Ar ratios; a), and the N deficit (b; calculated as $[NO_3^- + NO_2^-] - (N/P_{bw} * [PO_4^{3-}])$, with $N/P_{bw}$ being the average $NO_3^- + NO_2^-$, $PO_4^{3-}$ ratio seen in bottom waters during this cruise, which was assigned a value of 14). The $\delta^{15}N$ of nitrate, along with a depth profile of average nitrate concentrations (solid black line; grey shading shows upper and lower bounds) from all stations (c), and the $\delta^{18}O$ of nitrate (d). The dashed rectangle outlines the approximate depth interval where oxygen concentrations drop below 2.5 µM.

## Methods

Samples were collected at seven stations (Table S4) in the Bay of Bengal between the 24th of January and 3rd of February 2014 onboard the ORV Sagar Kanya. Seawater samples were collected using Niskin bottles (4x30 L and 8x5 L) on a rosette containing a Conductivity Temperature Depth (CTD) profiler (SBE 9/11 – SeaBird Electronics). The CTD was furthermore equipped with a SBE 43 oxygen sensor (see below) and WET Labs ECO-AFL/FL chlorophyll sensor. A complete array of samples, hydrographic, molecular, nutrients, geochemical and rate measurements were undertaken at stations 1, 4, and 5. At station 6, hydrographic, nutrient, geochemical and a reduced number of rate measurements were sampled for. Only hydrographic and a reduced number of rate measurements were undertaken at station 7 and, at stations 2 and 3 hydrographic profiles only.

### *In situ* $O_2$ measurements

Concentrations of oxygen were measured *in situ* with two methods. In order to assess the possibility of true anoxia in BoB waters we used STOX (Switchable Trace amount OXygen) amperometric oxygen[33] sensors mounted to a CTD frame. The signal from the STOX sensor was recorded on a custom-made Trace oxygen profiler (TOP)[34], consisting of a 16-bit A/D converter (DT9818, Data translation) controlled by a single board computer (fit-PC2i, CompuLab) housed in a titanium cylinder. The amplification of the STOX sensor signal was performed by a custom-made amplifier and the operation of the sensor switching was controlled by a cyclic switch operating with a 40 s on/off cycle. Data was sampled at 60 $s^{-1}$, filtered using 1.5 $s^{-1}$ low-pass filter, smoothed using a 5 s moving average and finally down-sampled to 1 $s^{-1}$. The detection limit of the STOX sensors in the given configuration was estimated to be 7-12 nM based on three times the standard deviations of the noise recorded in the zero signal. Calibration and calculations were performed as described previously[33, 35].

STOX measurements were performed at Stations 1,4,5,6 and 7. At Station 1, STOX measurements were only preformed to a depth of 270 m, due to a software error. The STOX data were recorded during the up-cast (except at Station 1) and the majority of the data were recorded while the instrument was moving. Additionally, several recordings were performed while the instrument was kept at a given depth for 3-5 min. These data are not distinguishable from data recorded as the CTD moved. All STOX oxygen data are presented in Table S1.

We also measured oxygen with the SBE 43 polarographic oxygen sensor mounted on the CTD. The data from the CTD was sampled at 24 $s^{-1}$, low-pass filtered at 0.15 $s^{-1}$ and down sampled to 1 $s^{-1}$. Only data

from the up-cast was used, as typical for oxygen measurements in OMZs (e.g.[35]), and casts were performed with a CTD speed of approximately 1 m $s^{-1}$ below 100 m and 0.5 m $s^{-1}$ above 100 m. The data from the SBE 43 and STOX were aligned using the pressure data recorded by both instruments.

When compared, the data from the SeaBird and STOX sensors showed excellent linearity (Figure S2), but with a positive offset on the order of 400 to 500 nM in the SeaBird oxygen reading. In principle we could have used this offset to calibrate the Seabird data to the STOX data, but when doing so, we found that the SeaBird sensor produced a large number of negative readings at the lowest oxygen levels. Since the STOX sensor clearly showed the persistence of oxygen in the OMZ, we elected instead to align the lowest readings on the SeaBird sensor with the readings from the same depth from the STOX sensor. This ensured that the Seabird readings were always positive values, and the offset ranged from 380 nM to 450 nM at the different sites.

**DNA sampling and methods**

Samples for molecular biological work were collected at Stations 1, 4, and 5 at water depths ranging from 10 m to 2300 m. Between 5 and 27 L of water per depth was filtered through a 3 µm pre-filter prior to a 0.22 µm Supor® PES membrane disc filter (PALL) on which we collected material for DNA analysis. Each membrane was stored in 2.7 mL sucrose lysis buffer (SLB) at -20ºC until DNA extraction.

*DNA extraction*

DNA was extracted after a modified version of the phenol:chloroform extraction[36]. Membranes in 2.7 mL SLB were allowed to thaw at room temperature. After addition of 150 µL of lysozyme (20 mg/ml) tubes were incubated at 37 ºC for 30 min under constant rotation. After this, 150 µL 20% (w/v) sodium dodecyl sulfate and 150 µL of proteinase K (20 mg/ml) were added and tubes were incubated at 55 °C for 120 min under continuous mixing. Nucleic acids were extracted with 1 volume phenol:chloroform:isoamylalcohol (IAA) (25:24:1) followed by centrifugation at 2,500 relative centrifugal force (rcf) for 10 min. The remaining phenol was extracted by 1 volume chloroform:IAA (24:1) followed by a centrifugation at 2,500 rcf for 5 min. Genomic DNA was precipitated with 0.1 volume of 3 M sodium acetate and 2-3 volumes of 96% ethanol, incubation at -20 °C for 8 hr. DNA was pelleted at 14,000 rcf for 45 min at 4 ºC and washed with 70% ice-cold ethanol and centrifuged at 14,000 rcf for 30 min at 4 ºC. The DNA was air dried at RT and resuspended in 100 µL preheated TE

buffer (60 ºC; pH 7.5). DNA concentrations, quality, and purity were checked spectrophotometrically (NanoDrop) and by the Quant-iT™ PicoGreen® dsDNA kit (Invitrogen).

*qPCR*

Copy numbers of 16S rRNA genes and functional genes were determined by qPCR using primer sets, concentrations, and specific conditions listed in Table S3. Each 20 µL reaction contained 10 µL SsoAdvanced™ SYPER® Green Supermix (Bio-Rad), 1-8 ng of template DNA and was adjusted to 20 µL final volume with nuclease-free water. Reactions were carried out in clear 96 Multiply® PCR plates (Sarstedt) and performed on a CFX Connect Real-Time System (Bio-Rad) running CFX Manager™ Software V3.0. General conditions were as follows: 98 ºC for 2 min followed by 40 cycles of 98 ºC for 5 s, listed annealing temperature for 15 s, 72 ºC for 15 s and a plate read. Finally, a melt curve from 65 ºC to 95 ºC held at each 0.5 ºC for 5 sec was performed to check the specificity of the reaction.

All reactions were run alongside standard curves of the corresponding gene ranging from $10^1$ to $10^7$ copies per µL. Mean PCR efficiencies for the standard curves are listed in Table S3 ($R^2$ values were all >0.99). Standards for each target gene were derived from clone libraries prepared from environmental samples with the same primers that were used for the qPCR.

**Nutrients**

Nitrate, nitrite and phosphate concentrations were determined following methods outlined in[37]. The nitrogen deficit was calculated as $[NO_3^- + NO_2^-] – (N/P_{bw} * [PO_4^{3-}])$, with $N/P_{bw}$ being the average $NO_3^- + NO_2^-$, $PO_4^{3-}$ ratio seen in bottom waters during this cruise, which was 14. Nutrient data is presented in Table S4. It is important to note here the weakness in using the N deficit in these waters. The various source waters, water masses, riverine input, and monsoonal rains are poorly constrained, and likely have varying N/P ratios, which could impact the N deficit calculation.

**Excess $N_2$: Sampling and Analysis**

Samples for high precision $N_2$/Ar measurements for the determination of biogenic $N_2$ were collected and analyzed following the protocol outlined in ref[38]. Samples were collected bubble-free in 60mL serum bottles, preserved with 100 µL of saturated $HgCl_2$ and stored at ambient temperature until analysis. Analyses were carried out on a custom-made on-line gas extraction system coupled to a multicollector IRMS (GV Isoprime). Oxygen was removed during gas purification by a hot copper furnace to avoid artifacts associated with varying $N_2/O_2$. Calibration was achieved through reference gas injections

($N_2$+Ar) and air equilibrated water standards of known temperature and salinity[38]. To assess the contribution from biogenically produced $N_2$ an additional background correction was applied. This was done by subtracting values from waters uninfluenced by N loss processes[39, 40]. In our study, no stations outside of the low-oxygen region were sampled, so background data was taken from the WOCE 107N line[39, 40].

Samples collected at depth (temperature 3 to 10 ºC) showed unusually high excess $N_2$. Increases with depth may be expected due to bubble injection during water mass formation[41], but should have been accounted for within the background correction. Samples were analyzed within 4 months of collection, at which time the integrity of the excess $N_2$ measurements should not have been compromised based on sample longevity tests[38]. However the longevity tests were conducted with storage at room temperature and not elevated and fluctuating temperatures as our samples likely experienced during transport. Storage effects will be highly dependent on the temperature difference between that observed in situ and that experienced during storage. As temperature in the open ocean has a clear monotonic distribution, we therefore also expect the residual excess $N_2$ as a result of storage to follow a similar distribution whereas a peak of excess $N_2$ in the shallower, warmer, low oxygen waters would suggest a biogenic signature from processes occurring in situ. Results are presented in Table S4.

**Nitrate Isotopes**

Samples for $\delta^{15}N_{NO3}$ ($\delta^{15}N$ (‰ vs. atmospheric $N_2$) = $[(^{15}N/^{14}N)_{NO3}/(^{15}N/^{14}N)_{N2}-1] \times 1000$) and $\delta^{18}O_{NO3}$ ($\delta^{18}O$ (‰ vs. VSMOW) = $[(^{18}O/^{16}O)_{NO3}/(^{18}O/^{16}O)_{VSMOW}-1] \times 1000$) were collected in 60mL acid-washed HDPE bottles and stored frozen until analysis. Samples were analyzed by cadmium reduction to $NO_2^-$ followed by reduction to $N_2O$ with azide[42, 43]. Pre-existing $NO_2^-$ was removed by adding sulfamic acid[44] prior to cadmium reduction. International standards IAEA-N3, USGS-34 and USGS-35[45] were used for calibration. Reproducibility was 0.3 and 0.5 ‰ for $\delta^{15}N_{NO3}$ and $\delta^{18}O_{NO3}$ respectively. Results are presented in Table S4.

**Process rate experiments**

Rates of microbial nitrogen turnover were determined using $^{15}N$ labeled substrates. Experiments were carried out at six depths at stations 1, 4 and 5 and at three depths at stations 6 and 7, following the methods outlined in refs[46, 47]. For each incubation, a 250 mL serum bottle was filled directly from the Niskin bottle and overflowed for at least three volume changes, then immediately capped with a butyl rubber stopper and crimped with an aluminum cap. Bottles were stored in the dark at *in situ* temperature

until all depths were collected. After this, bottles were purged with helium for 15 min and amended with $^{15}N$-labeled substrates during the purging. Four amendments were made: 1) 5μM $^{15}NH_4^+$, 2) 5μM $^{15}NO_2^-$ + 5μM $^{14}NH_4^+$, 3) 5μM $^{14}NO_2^-$ + 5μM $^{15}NH_4^+$ and 4) 25μM $^{15}NO_3^-$ (only amendments 2 and 3 were carried out at stations 6 and 7). $^{15}N$-amended samples were transferred into 12 mL exetainers (LabCo, UK), and capped with helium degassed caps to avoid oxygen contamination[48]. Exetainers were incubated in the dark at *in situ* temperature. At each time point (approximately 0, 3, 6, 12 and 24 hr), microbial activity was terminated in a single exetainer by the addition of 100 μL of saturated mercuric chloride solution. It is worthwhile to note that although the incubation approach used here was originally intended to yield anoxic conditions, the introduction of highly sensitive oxygen sensors have revealed that slight oxygen contamination is essentially unavoidable [49, 50].

The production of $^{14}N^{15}N$ and $^{15}N^{15}N$ was determined on a gas-chromatography isotope ratio mass spectrometer (GC-IRMS; VG Optima, Manchester, UK). The production of nitrite was determined from samples amended with $^{15}NO_3^-$ according to ref[47] with conversion to $N_2$ and determination of $^{14}N^{15}N$ by GC-IRMS (customized TraceGas coupled to a multicollector IsoPrime100, Manchester, UK). Rates for all processes were evaluated from the slope of the linear regression of $^{14}N^{15}N$ and/or $^{15}N^{15}N$ with time, correcting for the $^{15}N$ labeling percentages of the initial substrate pool. Rates of $N_2$ production by anammox and denitrification were calculated according to the equations in ref[51]. T-tests were applied in all cases to determine whether rates were significantly different from zero ($p < 0.05$). Detection limits varied from experiment to experiment and were estimated from the median of the standard error of the slope, multiplied by the t value for $p = 0.05$. Thus, the median detection limits for anammox were 1.3 and 2.2 nM N $d^{-1}$ for $^{15}NH_4^+$ and $^{15}NO_2^-$ incubations, 2.7 nM N $d^{-1}$ for denitrification ($^{15}NO_2^-$ incubation) and 3.0 nM N $d^{-1}$ for nitrate reduction ($^{15}NO_3^-$ incubation; anammox and denitrification rates were all non-significant with $^{15}NO_3^-$ amendments).

**Oxygen Regulation Experiments**

Water for oxygen regulation experiments was sampled immediately after the Niskin bottles arrived on deck and transferred to a 20 L glass bottle. The bottle was overflowed (at least two volume equivalents) and sealed without bubbles using deoxygenated butyl rubber stoppers[48], then stored in the dark at *in situ* temperature until the experiment began. The bottle was spiked with $^{15}NO_2^-$ to a final concentration of 5 μM and then degassed with helium (~ 1 hr). At this point, the water was dispensed into custom-modified Schott Duran glass bottles (1160 mL) as described in ref[52]. An additional modification was the

placement of a third glass port on the bottle, which held a 100 mL glass reservoir filled with sample water, that was continually degassed with helium for the duration of the experiment. During the incubations the bottles were continuously stirred[52], kept in the dark, and submersed in a water bath to maintain *in situ* temperature. Oxygen additions were made by injecting known volumes of air-saturated seawater. In this setup, oxygen was monitored throughout the incubations using a highly sensitive optical trace oxygen optode and readout device[50], mounted on the side of the bottle. Sensors were individually calibrated after each experiment, with zero point calibrations using a 0.1% w/v sodium-dithionite solution.

Time-series sampling was undertaken at 0, 4, 8, 12 and 16 hr, by inserting a long needle down the pressure compensation tube, opening the reservoir and withdrawing 10mL of sample. Sample was injected into 6 mL exetainers (LabCo, UK), pre-spiked with 50 µL 50% w/v $ZnCl_2$. Analysis of $^{14}N^{15}N$ and $^{15}N^{15}N$ for $N_2$ production rates were performed on a gas chromatography isotope ratio mass spectrometer as in [53]. Anammox and denitrification rates were determined using the equations presented in ref[51].

Nitrite oxidation was determined from the production of $^{15}NO_3^-$. After the removal of residual $^{15}NO_2^-$ with sulfamic acid, $^{15}NO_3^-$ was converted to $^{15}NO_2^-$ by cadmium reduction and then to $N_2$ with sulfamic acid[42, 47]. Process rates were calculated from the linear regression of $^{14}N^{15}N$ and/or $^{15}N^{15}N$ as a function of time. T-tests were applied in all cases to determine whether rates were significantly different from zero ($p < 0.05$). Detection limits for the oxygen regulation experiments were estimated from the median of the standard error of the slope, multiplied by the t value for $p = 0.05$. Detection limits vary from experiment to experiment, but median detection limits were 0.9 nM N $d^{-1}$ for anammox in $^{15}NO_2^-$ incubations, 0.4 nM N $d^{-1}$ for denitrification and 6.3 nM N $d^{-1}$ for nitrite oxidation. Data from these experiments are shown in Table S2.

**Data Availability**

The authors declare that data supporting the findings of this study are available within this article and its supplementary information, and all additional data are available from the corresponding author upon request.

**Methods References**


33. Revsbech NP, Larsen LH, Gundersen J, Dalsgaard T, Ulloa O, Thamdrup B. Determination of ultra-low oxygen concentrations in oxygen minimum zones by the STOX sensor. *Limnology and Oceanography: Methods* 2009, **7:** 371-381.

34. Larsen M, Lehner P, Borisov SM, Klimant I, Fischer JP, Stewart FJ*, et al.* In situ quantification of ultra-low O2 concentrations in oxygen minimum zones: Application of novel optodes. *Limnology and Oceanography: Methods* 2016**:** n/a-n/a.

35. Thamdrup B, Dalsgaard T, Revsbech NP. Widespread functional anoxia in the oxygen minimum zone of the Eastern South Pacific. *Deep-Sea Research Part I-Oceanographic Research Papers* 2012, **65:** 36-45.

36. Giovannoni SJ, Rappe MS, Vergin KL, Adair NL. 16S rRNA genes reveal stratified open ocean bacterioplankton populations related to the Green Non-Sulfur bacteria. *Proceedings of the National Academy of Sciences of the United States of America* 1996, **93**(15)**:** 7979-7984.

37. Grasshoff K, Kremling K, Ehrhardt M. *Methods of Seawater Analysis*, 3rd edn. Wiley-VCH: New York, 1999.

38. Charoenpong CN, Bristow LA, Altabet MA. A continuous flow isotope ratio mass spectrometry method for high precision determination of dissolved gas ratios and isotopic composition. *Limnology and Oceanography-Methods* 2014, **12:** 323-337.

39. Devol AH, Uhlenhopp AG, Naqvi SWA, Brandes JA, Jayakumar DA, Naik H*, et al.* Denitrification rates and excess nitrogen gas concentrations in the Arabian Sea oxygen deficient zone. *Deep-Sea Research Part I-Oceanographic Research Papers* 2006, **53**(9)**:** 1533-1547.

40. Chang BX, Devol AH, Emerson SR. Fixed nitrogen loss from the eastern tropical North Pacific and Arabian Sea oxygen deficient zones determined from measurements of N-2:Ar. *Global Biogeochemical Cycles* 2012, **26**.

41. Hamme RC, Emerson SR. Mechanisms controlling the global oceanic distribution of the inert gases argon, nitrogen and neon. *Geophysical Research Letters* 2002, **29**(23).

42. McIlvin MR, Altabet MA. Chemical conversion of nitrate and nitrite to nitrous oxide for nitrogen and oxygen isotopic analysis in freshwater and seawater. *Analytical Chemistry* 2005, **77**(17)**:** 5589-5595.

43. Ryabenko E, Altabet MA, Wallace DWR. Effect of chloride on the chemical conversion of nitrate to nitrous oxide for delta N-15 analysis. *Limnology and Oceanography-Methods* 2009, **7:** 545-552.

44. Granger J, Sigman DM. Removal of nitrite with sulfamic acid for nitrate N and O isotope analysis with the denitrifier method. *Rapid Communications in Mass Spectrometry* 2009, **23**(23)**:** 3753-3762.

45. Bohlke JK, Mroczkowski SJ, Coplen TB. Oxygen isotopes in nitrate: new reference materials for O-18 : O-17 : O-16 measurements and observations on nitrate-water equilibration. *Rapid Communications in Mass Spectrometry* 2003, **17**(16)**:** 1835-1846.

46. Holtappels M, Lavik G, Jensen MM, Kuypers MMM. N-15-LABELING EXPERIMENTS TO DISSECT THE CONTRIBUTIONS OF HETEROTROPHIC DENITRIFICATION AND ANAMMOX TO NITROGEN REMOVAL IN THE OMZ WATERS OF THE OCEAN. In: Klotz MG (ed). *Methods in Enzymology: Research on Nitrification and Related Processes, Vol 486, Part A*, vol. 486. Elsevier Academic Press Inc: San Diego, 2011, pp 223-251.

47. Füssel J, Lam P, Lavik G, Jensen MM, Holtappels M, Gunter M*, et al.* Nitrite oxidation in the Namibian oxygen minimum zone. *Isme Journal* 2012, **6**(6)**:** 1200-1209.

48. De Brabandere L, Thamdrup B, Revsbech NP, Foadi R. A critical assessment of the occurrence and extend of oxygen contamination during anaerobic incubations utilizing commercially available vials. *Journal of Microbiological Methods* 2012, **88**(1)**:** 147-154.

49. Ganesh S, Bristow LA, Larsen M, Sarode N, Thamdrup B, Stewart FJ. Size-fraction partitioning of community gene transcription and nitrogen metabolism in a marine oxygen minimum zone. *ISME J* 2015.

50. Lehner P, Larndorfer C, Garcia-Robledo E, Larsen M, Borisov SM, Revsbech N-P*, et al.* LUMOS - A Sensitive and Reliable Optode System for Measuring Dissolved Oxygen in the Nanomolar Range. *PLoS ONE* 2015, **10**(6)**:** e0128125.

51. Thamdrup B, Dalsgaard T. Production of $N_2$ through anaerobic ammonium oxidation coupled to nitrate reduction in marine sediments. *Applied and Environmental Microbiology* 2002, **68:** 1312-1318.

52. Tiano L, Garcia-Robledo E, Dalsgaard T, Devol AH, Ward BB, Ulloa O*, et al.* Oxygen distribution and aerobic respiration in the north and south eastern tropical Pacific oxygen minimum zones. *Deep-Sea Research Part I-Oceanographic Research Papers* 2014, **94:** 173-183.

53. Dalsgaard T, Thamdrup B, Farias L, Revsbech NP. Anammox and denitrification in the oxygen minimum zone of the eastern South Pacific. *Limnology and Oceanography* 2012, **57**(5)**:** 1331-1346.

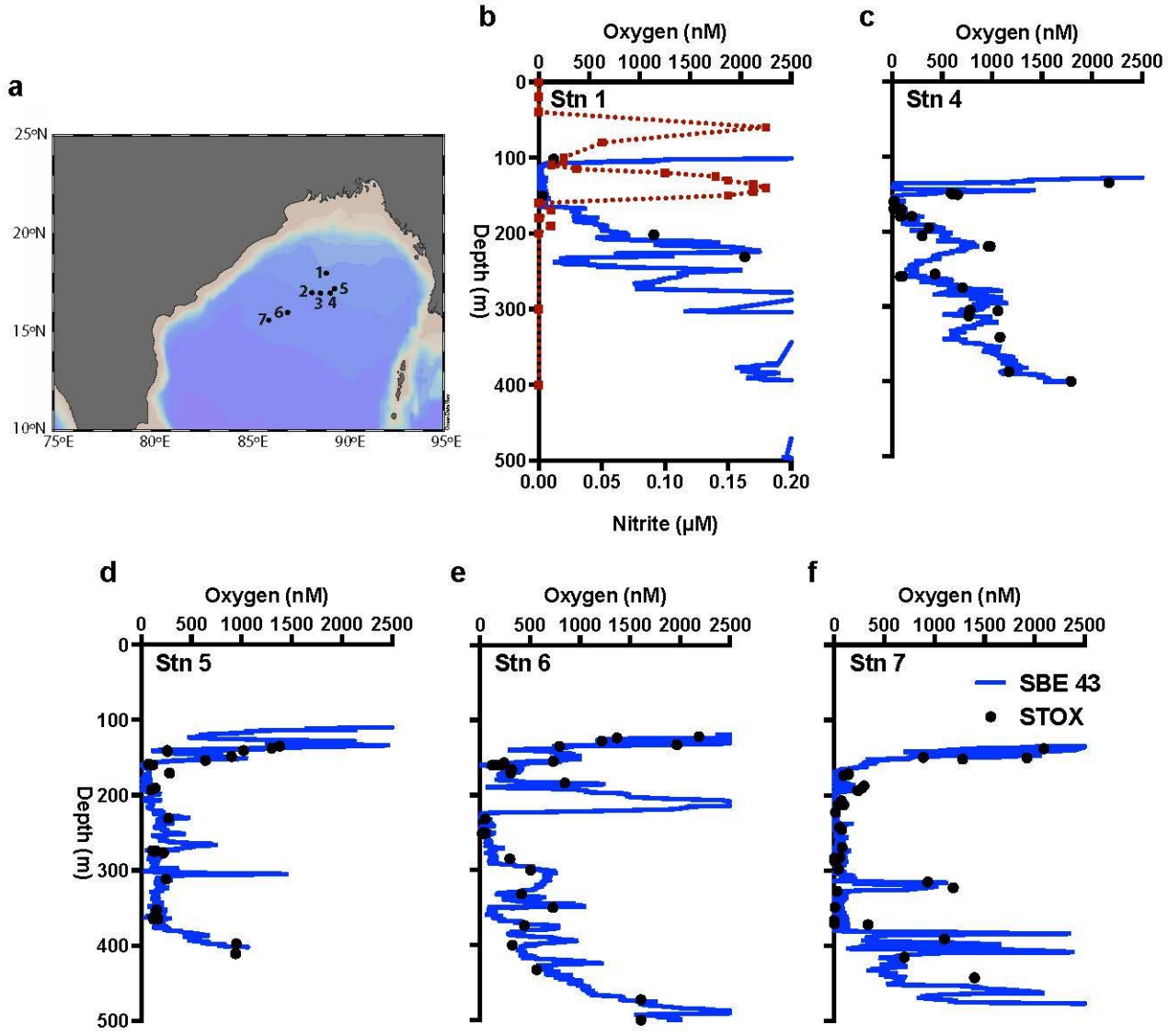
a
25°N
20°N
15°N
10°N
75°E
80°E
85°E
90°E
95°E
1
2
3
4
5
6
7
b
Oxygen (nM)
0 500 1000 1500 2000 2500
Stn 1
Depth (m)
0 100 200 300 400 500
0.00 0.05 0.10 0.15 0.20
Nitrite (μM)
c
Oxygen (nM)
0 500 1000 1500 2000 2500
Stn 4
d
Oxygen (nM)
0 500 1000 1500 2000 2500
Stn 5
Depth (m)
0 100 200 300 400 500
e
Oxygen (nM)
0 500 1000 1500 2000 2500
Stn 6
f
Oxygen (nM)
0 500 1000 1500 2000 2500
Stn 7
SBE 43
STOX

**Figure -1**

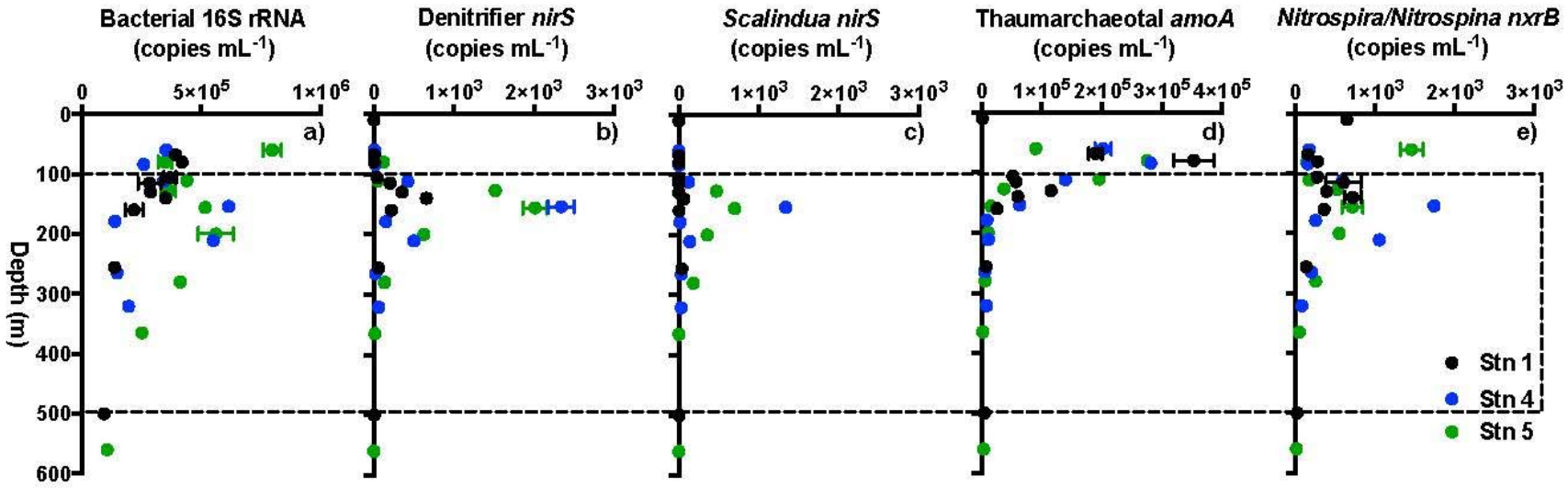
Bacterial 16S rRNA
(copies mL-1)
Denitrifier nirS
(copies mL-1)
Scalindua nirS
(copies mL-1)
Thaumarchaeotal amoA
(copies mL-1)
Nitrospira/Nitrospina nxrB
(copies mL-1)
a)
b)
c)
d)
e)
Depth (m)
Stn 1
Stn 4
Stn 5

**Figure -2**

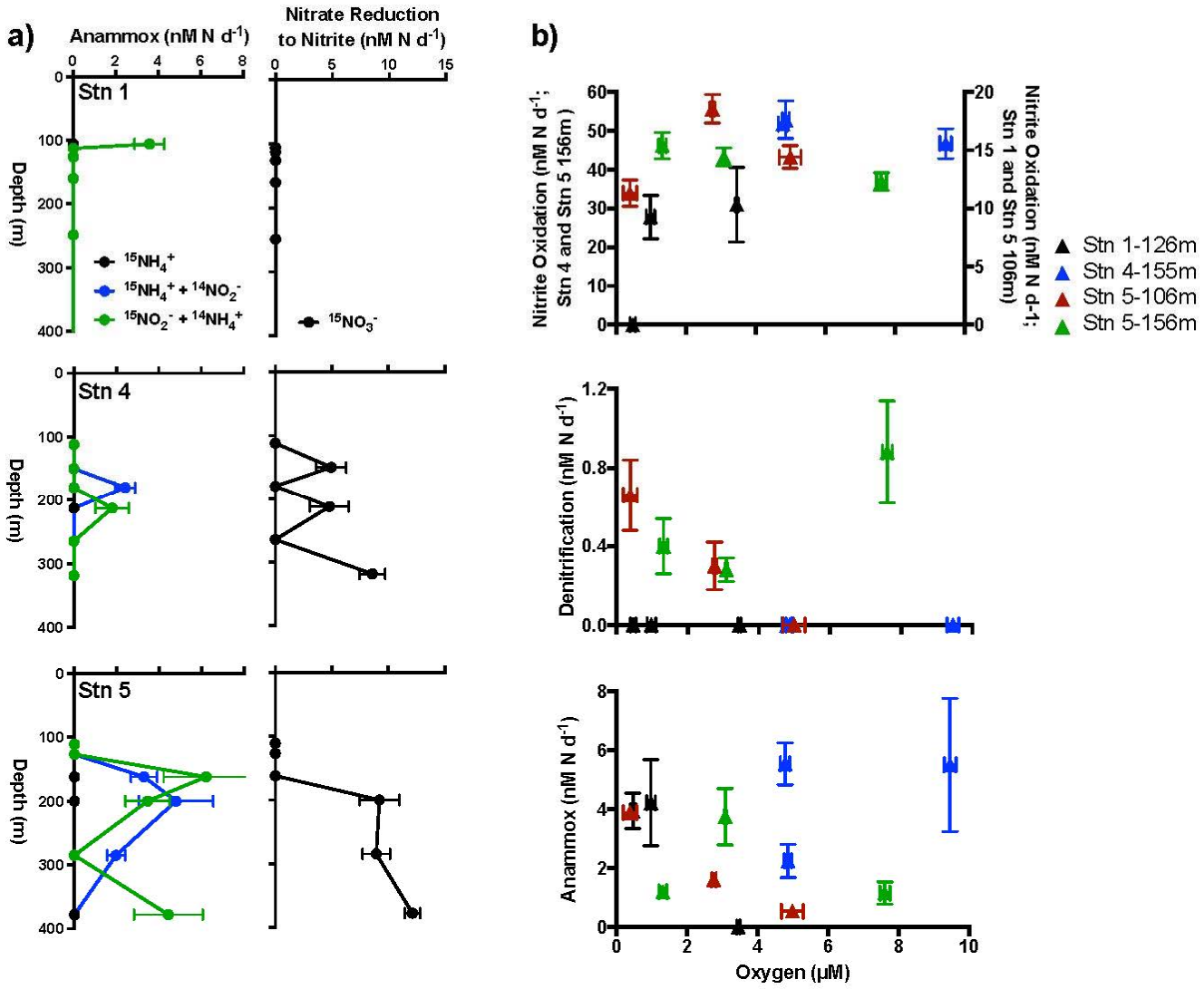
a)
Anammox (nM N d-1)
Nitrate Reduction to Nitrite (nM N d-1)
Stn 1
Stn 4
Stn 5
Depth (m)
15NH4+
15NH4+ + 14NO2-
15NO2- + 14NH4+
15NO3-
b)
Nitrite Oxidation (nM N d-1; Stn 4 and Stn 5 156m)
Nitrite Oxidation (nM N d-1; Stn 1 and Stn 5 106m)
Stn 1-126m
Stn 4-155m
Stn 5-106m
Stn 5-156m
Denitrification (nM N d-1)
Anammox (nM N d-1)
Oxygen (µM)

**Figure - 3**

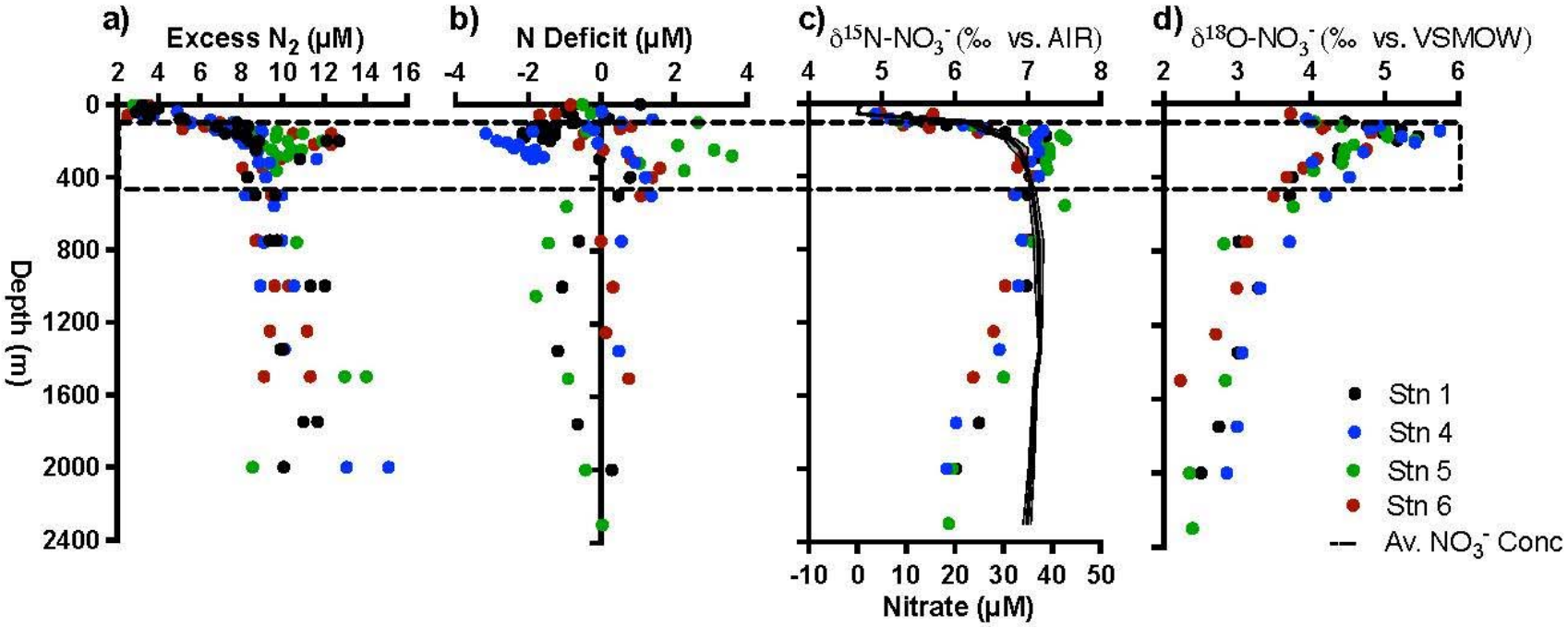
a)
Excess $N_2$ (µM)
2 4 6 8 10 12 14 16
b)
N Deficit (µM)
-4 -2 0 2 4
c)
$\delta^{15}N\text{-}NO_3^-$ (‰ vs. AIR)
4 5 6 7 8
d)
$\delta^{18}O\text{-}NO_3^-$ (‰ vs. VSMOW)
2 3 4 5 6
Depth (m)
0
400
800
1200
1600
2000
2400
-10 0 10 20 30 40 50
Nitrate (µM)
Stn 1
Stn 4
Stn 5
Stn 6
Av. $NO_3^-$ Conc

**Figure - 4**